

Magnetic Order in $\text{TbCo}_2\text{Zn}_{20}$ and $\text{TbFe}_2\text{Zn}_{20}$

W. Tian,¹ A. D. Christianson,² J. L. Zarestky,¹ S. Jia,^{1,*} S. L. Bud'ko,¹ P. C. Canfield,¹ P. M. B. Piccoli,³ and A. J. Schultz³

¹*Ames Laboratory and Department of Physics and Astronomy, Iowa State University, Ames, Iowa 50011, USA*

²*Oak Ridge National Laboratory, Oak Ridge, TN 37831, USA*

³*Argonne National Laboratory, Argonne, IL 60439, USA*

We report neutron diffraction studies of $\text{TbCo}_2\text{Zn}_{20}$ and $\text{TbFe}_2\text{Zn}_{20}$, two isostructural compounds which exhibit dramatically different magnetic behavior. In the case of $\text{TbCo}_2\text{Zn}_{20}$, magnetic Bragg peaks corresponding to antiferromagnetic order are observed below $T_N \approx 2.5$ K with a propagation vector of $(0.5 \ 0.5 \ 0.5)$. On the other hand, $\text{TbFe}_2\text{Zn}_{20}$ undergoes a ferromagnetic transition at temperatures as high as 66 K which shows a high sensitivity to sample-to-sample variations. Two samples of $\text{TbFe}_2\text{Zn}_{20}$ with the same nominal compositions but with substantially different magnetic ordering temperatures ($T_c \approx 51$ and 66 K) were measured by single crystal neutron diffraction. Structural refinements of the neutron diffraction data find no direct signature of atomic site disorder between the two $\text{TbFe}_2\text{Zn}_{20}$ samples except for subtle differences in the anisotropic thermal parameters. The differences in the anisotropic thermal parameters between the two samples is likely due to very small amounts of disorder. This provides further evidence for the extreme sensitivity of the magnetic properties of $\text{TbFe}_2\text{Zn}_{20}$ to small sample variations, even small amounts of disorder.

PACS numbers: valid numbers to be inserted here

I. INTRODUCTION

The $\text{RT}_2\text{Zn}_{20}$ (R = Rare Earth and T = Transition metal) family of materials exhibit diverse magnetic properties^{1–5}. For example, nearly ferromagnetic Fermi liquid behaviour was observed in $\text{YFe}_2\text{Zn}_{20}$ ¹ and $\text{LuFe}_2\text{Zn}_{20}$ ⁵. Subsequently it was shown that by substituting a small amount of Y by Gd the $\text{Gd}_x\text{Y}_{1-x}\text{Fe}_2\text{Zn}_{20}$ system becomes ferromagnetic for $x > 0.02$ ³ and a remarkably high ferromagnetic ordering temperature of $T_c = 86$ K is found for $\text{GdFe}_2\text{Zn}_{20}$ ¹. Moreover, six closely related Yb-based heavy fermion compounds were discovered in $\text{YbT}_2\text{Zn}_{20}$ for T = Fe, Ru, Os, Co, Rh and Ir² that significantly increase the total number of Yb-based heavy fermion materials. The exotic magnetic properties discovered in recent studies have generated great interest in the $\text{RT}_2\text{Zn}_{20}$ compounds.

The $\text{RT}_2\text{Zn}_{20}$ materials crystallize in the cubic $\text{CeCr}_2\text{Al}_{20}$ type structure ($Fd\bar{3}m$ space group). The R and T ions each occupy a unique crystallographic site, $8a$ and $16d$ respectively, whereas the Zn ions have three distinct crystallographic sites, $96g$, $48f$ and $16c$ ^{6,7}. Even though these materials are comprised of more than 85% Zn, they are highly tunable and ideal for fundamental research such as magnetism for two reasons. (1) As illustrated in Fig. 1, the R and T ions are surrounded exclusively by Zn atoms and there are no R-R, R-T, and T-T nearest neighbors in the system; (2) Due to the very low R concentrations in these compounds (less than 5 at.%), the local environment of the R site is only weakly affected by the changing of T. Thus by substituting on either the rare-earth site or the transition metal site, these isostructural compounds can serve as model systems for a variety of physical phenomenon.

Among the $\text{RT}_2\text{Zn}_{20}$ compounds, $\text{GdFe}_2\text{Zn}_{20}$ and $\text{GdCo}_2\text{Zn}_{20}$ have attracted special attention due to the

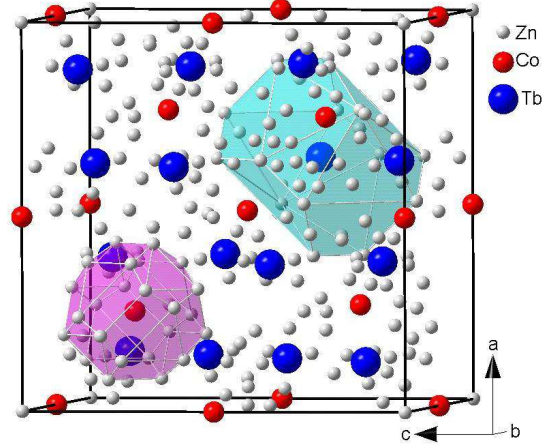


FIG. 1: (Color online) The schematic crystal structure of $\text{TbCo}_2\text{Zn}_{20}$ shows that both Tb and Co ions are surrounded exclusively by Zn atoms as illustrated by the coordination polyhedron of Tb (cyan) and Co (pink).

distinct magnetic properties exhibited by each material¹. $\text{GdFe}_2\text{Zn}_{20}$ is a ferromagnet with a remarkably high ordering temperature of $T_c = 86$ K. However, upon substitution of Co for Fe, ferromagnetism is rapidly suppressed⁴ culminating in antiferromagnetic order at $T_N = 5.7$ K in $\text{GdCo}_2\text{Zn}_{20}$. Band structure calculations suggest that the enhanced magnetic ordering temperature in $\text{GdFe}_2\text{Zn}_{20}$ is due to a large d-electron contribution to the electronic density of states when compared to $\text{GdCo}_2\text{Zn}_{20}$. In addition to sensitivity to transition metal substitution, $\text{GdFe}_2\text{Zn}_{20}$ exhibits sensitivity to small sample-to-sample variations. Similar behavior has also been observed in Sc_3In and ZrZn_2 , materials on

the ferromagnetic side just over the Stoner limit⁸⁻¹⁰.

To provide further information concerning the microscopic origin of the magnetic behavior in the $\text{RT}_2\text{Zn}_{20}$ family we have performed neutron scattering measurements on $\text{TbFe}_2\text{Zn}_{20}$ and $\text{TbCo}_2\text{Zn}_{20}$. $\text{TbFe}_2\text{Zn}_{20}$ and $\text{TbCo}_2\text{Zn}_{20}$ are ideal for neutron scattering studies as these materials exhibit similar magnetic behavior to $\text{GdFe}_2\text{Zn}_{20}$ and $\text{GdCo}_2\text{Zn}_{20}$, but do not possess the strong neutron absorption cross-section of gadolinium. We have studied single crystalline and polycrystalline samples of $\text{TbCo}_2\text{Zn}_{20}$ and find antiferromagnetic order below $T_N \approx 2.5$ K with a propagation vector of $(0.5 \ 0.5 \ 0.5)$. Refinements of the magnetic structure indicate an ordered moment of $\sim 7.46 \mu_B$ at 1.4 K. In the case of ferromagnetic $\text{TbFe}_2\text{Zn}_{20}$ we investigated two single crystals prepared by slightly different methods that resulted in a ~ 15 K difference in ordering temperatures. No obvious signs of site disorder were detected in structural refinements of the neutron data, highlighting the extreme sensitivity to small sample variations. However, there are small differences in the refinements which suggest that the sample with the higher transition temperature is more highly ordered. The neutron scattering data are consistent with a picture of the $\text{RFe}_2\text{Zn}_{20}$ family where the high rare earth ordering temperatures are associated with the highly polarizable Fe lattice and are extremely sensitive to disorder.

II. EXPERIMENTAL DETAILS

$\text{TbFe}_2\text{Zn}_{20}$ and $\text{TbCo}_2\text{Zn}_{20}$ single crystals were grown from a Zn-rich self flux^{1,11} in the novel materials and ground states group at Ames Laboratory. Two methods, denoted method 1 and 2 were used to grow crystals of $\text{TbFe}_2\text{Zn}_{20}$: s1 and s2, respectively. The primary difference between methods 1 and 2 is that the initial molar ratios of the starting elements (Tb:Fe:Zn) were 2:5:95 and 2:3:93 respectively. The resulting single crystals have identical morphology and size to single crystals grown from the molar ratio of the starting elements R:T:Zn = 2:4:94 in Ref. 1. Although the magnetic ordering temperatures of the $\text{TbFe}_2\text{Zn}_{20}$ samples synthesized by methods 1 and 2 are different by ~ 15 K (see Fig. 4 below), single crystal x-ray diffraction measurements cannot fully resolve possible variations of occupancy of Fe and Zn sites, due to their similar atomic numbers.¹² The $\text{TbCo}_2\text{Zn}_{20}$ crystals were grown from the molar ratio of the starting elements Tb:Co:Zn = 2:4:94. The magnetic susceptibility of $\text{TbCo}_2\text{Zn}_{20}$ and $\text{TbFe}_2\text{Zn}_{20}$ were measured using a Quantum Design MPMS units whereas transport measurements on $\text{TbFe}_2\text{Zn}_{20}$ were made using Quantum Design PPMS.

Neutron diffraction measurements of $\text{TbCo}_2\text{Zn}_{20}$ were performed on a ~ 1.7 gram single crystal and ~ 2 gram powder using the HB1A triple axis spectrometer at the High Flux Isotope Reactor (HFIR) at the Oak Ridge National Laboratory (ORNL). The HB1A spectrometer

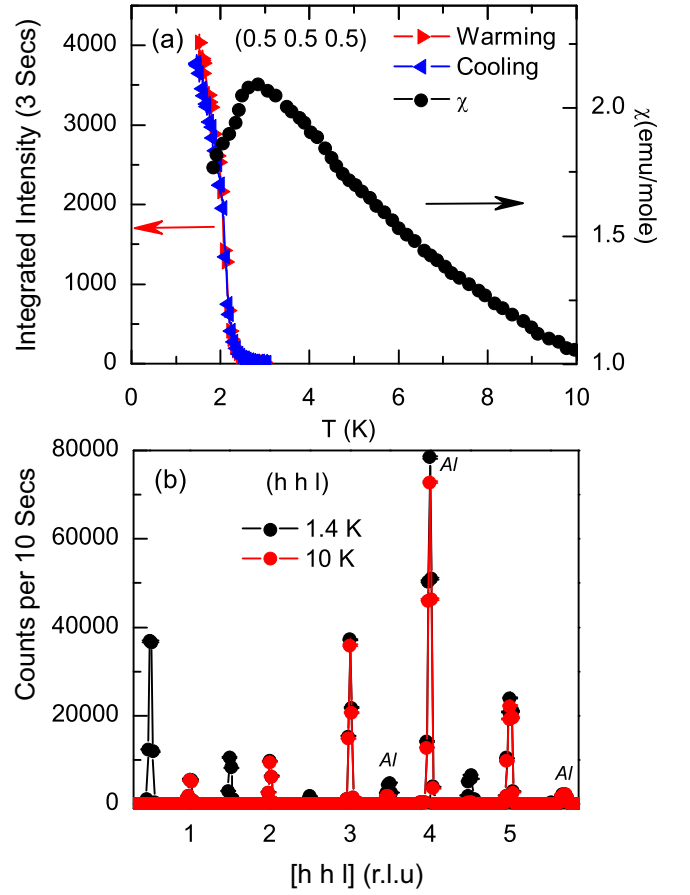


FIG. 2: (Color online) $\text{TbCo}_2\text{Zn}_{20}$ single crystal measurements with the crystal oriented in the (hhl) scattering plane. (a) Temperature dependence of the integrated scattering intensity of $(0.5 \ 0.5 \ 0.5)$ magnetic reflection (left) and the magnetic susceptibility (right) measured with $H \parallel [111]$ and $H = 0.1$ T. Note the temperature of onset magnetic scattering is close to the temperature (2.5 K) of maximal $d(\chi T)/dT$ value in Ref. 5. (b) Typical elastic long scans along the (hhl) direction measured at $T = 1.4$ K and $T = 10$ K, respectively. Aluminum reflection contributions ($2\theta = 60.79^\circ$, 71.5° , and 111.44°) from the aluminum sample holder are marked.

operates with a fixed incident energy of 14.64 meV using a double pyrolytic graphite (PG) monochromator system. The second-order contamination in the beam was removed ($I_{\lambda/2} \cong 10^{-4} I_\lambda$) by placing two PG filters located before and after the second monochromator. The $\text{TbCo}_2\text{Zn}_{20}$ single crystal was mounted on a aluminum plate and oriented in the (hhl) scattering plane. For low temperature measurements, both samples were sealed in an aluminum can under Helium atmosphere and cooled using a closed-cycle Helium refrigerator. A collimation of $48'-48'$ -sample- $40'-68'$ from reactor to detector was used throughout the measurements and all results shown have been normalized to a beam monitor count.

Two $\text{TbFe}_2\text{Zn}_{20}$ single crystals with the same nominal compositions hereafter denoted s1 and s2 were selected for neutron scattering measurements. The crystals were

TABLE I: Rietveld structure refinement results for $\text{TbCo}_2\text{Zn}_{20}$ at $T = 1.4$ K and 10 K.

Atom	site	T(K)	x	y	z
Tb	8a	10	0.125	0.125	0.125
Co	16d	10	0.5	0.5	0.5
Zn1	16c	10	0	0	0
Zn2	48f	10	0.4916(6)	0.125	0.125
Zn3	96g	10	0.0608(3)	0.0608	0.3245(5)
Lattice		10	$a=b=c=14.0358(3)$ Å; $V_{\text{cell}}=2765.104(8)$ Å ³ ;		
and			$R_{\text{Bragg}}=5.28$ %; $R_p=5.0$ %; $R_{wp}=6.4$ %; $\chi^2=1.4$;		
Reliability					
factors		1.4	$a=b=c=14.0290(2)$ Å; $V_{\text{cell}}=2761.09(8)$ Å ³ ;		
			$R_{\text{Bragg}}=8.35$ %;		
			$R_{\text{mag}}=13.86$ %; $R_p=13.8$ %; $R_{wp}=15.5$ %; $\chi^2=12.8$;		

cut to $\sim 3 \times 3 \times 3$ mm³ with sample masses of 0.213 g (s1) and 0.210 g (s2). The samples were mounted on aluminum pins with epoxy and attached to the cold finger of a standard closed cycle refrigerator. Neutron diffraction patterns were collected in a standard configuration of the SCD single-crystal neutron Laue Diffractometer at the Intense Pulsed Neutron Source (IPNS) at Argonne National Laboratory¹³. 10 crystal settings were selected to cover an octant of reciprocal space for each sample resulting in around 3600 reflections per sample. A counting time of 3 hours per crystal setting was used. Data were reduced with the ISAW package¹⁴ and corrected for neutron absorption. Structural refinements were done with the General Structural Analysis System (GSAS) software package¹⁵. Equivalent reflections have not been averaged since the extinction correction applied during the structural refinements is strongly wavelength dependent.

III. RESULTS

A. $\text{TbCo}_2\text{Zn}_{20}$

Figure 2(a) shows the magnetic susceptibility (right axis) of $\text{TbCo}_2\text{Zn}_{20}$ measured at $H = 0.1$ T with $H \parallel [111]$. A peak observed at $T \approx 2.8$ K with a maximal value of $d(\chi T)/dT$ found for $T \sim 2.5$ K⁵ suggests a magnetic, long-range order (LRO) transition near 2.5 K. To examine this low temperature phase, single crystal neutron diffraction measurements were carried out at temperatures above and below $T \approx 2.5$ K. Fig. 2 (b) compares two wave vector scans measured along the (hhl) direction at $T = 1.4$ K and 10 K. At $T = 1.4$ K, $(\frac{h}{2}, \frac{h}{2}, \frac{l}{2})$ (h, l are odd integers) type reflections were detected. The absence of these reflections at $T = 10$ K indicate they are magnetic in origin. To verify the observed magnetic reflections at 1.4 K are indeed associated with the $T \approx 2.5$ K phase transition, order parameter measurements were carried out by monitoring the strong (0.5 0.5) magnetic peak as a function of temperature between $T = 1.4$ K and $T = 10$ K. As shown in Fig. 2 (a), the

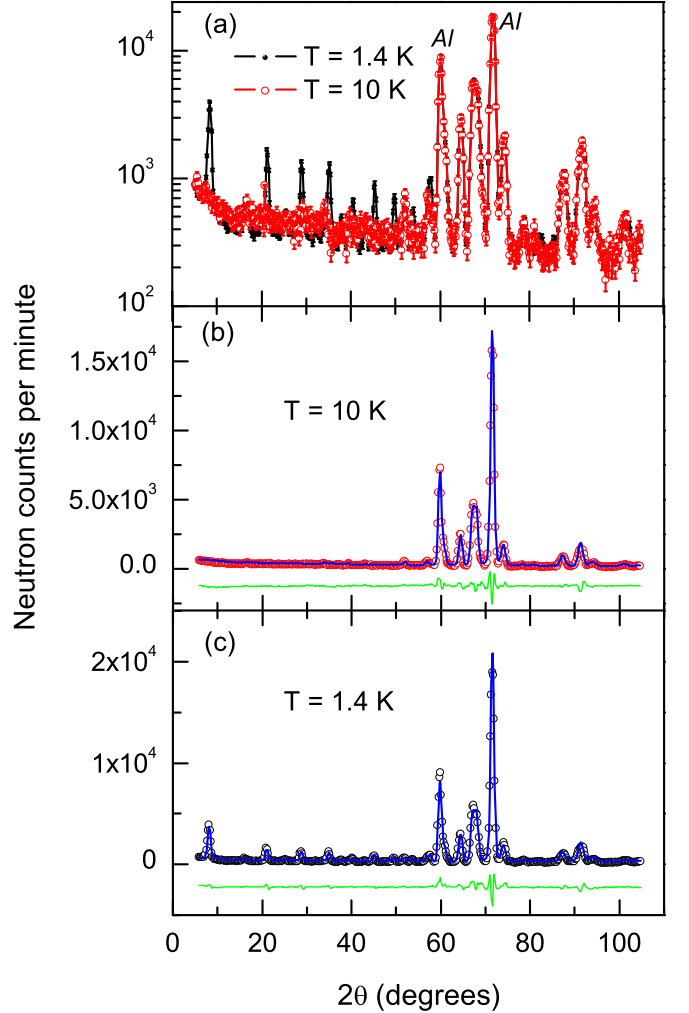


FIG. 3: (Color online) (a) Neutron powder diffraction patterns in log scale measured at $T = 1.4$ K (solid circles) and $T = 10$ K (open circles). Aluminum reflections ($2\theta = 60.79^\circ, 71.5^\circ$) from aluminum sample container are marked. Observed neutron powder diffraction pattern (circles), calculated profile (solid line) and their difference (bottom line) between $5 < 2\theta < 105$ measured at (b) $T = 10$ K, and (c) $T = 1.4$ K.

integrated intensity of (0.5 0.5 0.5) (right axis) increases rapidly at the transition temperature $T_N \approx 2.5$ K in good agreement with the magnetic susceptibility⁵. The single crystal measurements confirm that $\text{TbCo}_2\text{Zn}_{20}$ is a long-range ordered antiferromagnet.

To study the low temperature magnetic structure of $\text{TbCo}_2\text{Zn}_{20}$, ~ 2 grams powder were prepared by grinding single crystals. Powder diffraction data were collected over the range of $5^\circ < 2\theta < 165^\circ$ with a 2θ step size of 0.02° at 1.4 K & 10 K. As illustrated in Fig. 3 (a), multiple magnetic peaks were observed below T_N associated with the antiferromagnetic long range ordered phase. Consistent with the single crystal measurements, the observed magnetic peaks can be indexed as $(\frac{h}{2}, \frac{k}{2}, \frac{l}{2})$ (h, k, l are odd integers) suggesting the doubling of the magnetic unit cell along all three principle axis directions.

We carried out Rietveld refinements of the neutron data using the FULLPROF program¹⁶. The $T = 10$ K neutron powder data was first refined to check the nuclear crystal structure of $\text{TbCo}_2\text{Zn}_{20}$. The refinement results show (Fig. 3 (b)) that the crystal structure of $\text{TbCo}_2\text{Zn}_{20}$ belongs to the cubic $Fd\bar{3}m$ space group consistent with earlier studies. The refined lattice constants and atomic positions are given in Table I. To refine the $T = 1.4$ K low temperature data, the representation analysis technique¹⁷, program SARA¹⁸ and BasIreps (Rodriguez-Carvajal, 2004) were used as a tool to generate magnetic structures that are compatible with the $\text{TbCo}_2\text{Zn}_{20}$ crystal structure. There are four possible irreducible representations associated with the $Fd\bar{3}m$ space group as listed in table II. The labeling of the propagation vector and the irreducible representations in table II follows the scheme used by Kovalev¹⁹. Refinements of the $T = 1.4$ K data using FULLPROF indicates that the magnetic structure of $\text{TbCo}_2\text{Zn}_{20}$ can only be described by the irreducible representation Γ_5 . Figure 3(c) shows the refinement results considering both the magnetic and crystal structure unit cell. At $T = 1.4$ K, the refined magnetic moment of Tb^{3+} ion is $\sim 7.46 \mu_B$. We note that the moment has not yet saturated by 1.4 K thus the ordered moment at $T = 0$ K is probably somewhat closer to the full moment value of $K \sim 9.5 \mu_B$. Some reduction in the ordered moment is expected due to crystal field level splitting. Preliminary inelastic neutron scattering work suggests the crystal field level splitting of the Tb ground state multiplet in $\text{TbCo}_2\text{Zn}_{20}$ is less than 1.5 meV.

B. $\text{TbFe}_2\text{Zn}_{20}$

As noted above, two single crystals of $\text{TbFe}_2\text{Zn}_{20}$ (s1 and s2) were studied. Although s1 and s2 have the same nominal stoichiometry, an ~ 15 K difference in T_c was observed in thermodynamic and transport properties. The temperature dependence of the magnetization divided by applied field (M/H) (Fig. 4 (a)) and resistivity (Fig. 4 (b)) reveal a FM transition temperature $T_{c1} \approx 66 \pm 3$ K for s1 and $T_{c2} \approx 51 \pm 2$ K for s2 respectively.

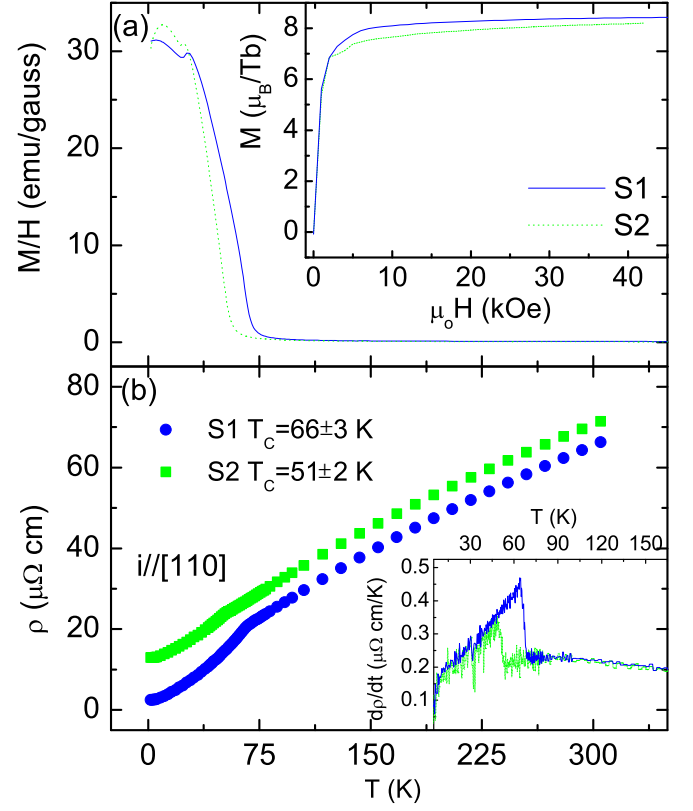


FIG. 4: (Color online) Physical properties of $\text{TbFe}_2\text{Zn}_{20}$ crystals, s1 and s2. (a) M/H as a function of temperature. Inset: Magnetization versus applied magnetic field H at $T = 2$ K with $H \parallel [111]$ (b) Electrical resistivity ρ as a function of temperature. Inset: $d\rho/dT$ between 1.5 K and 165 K.

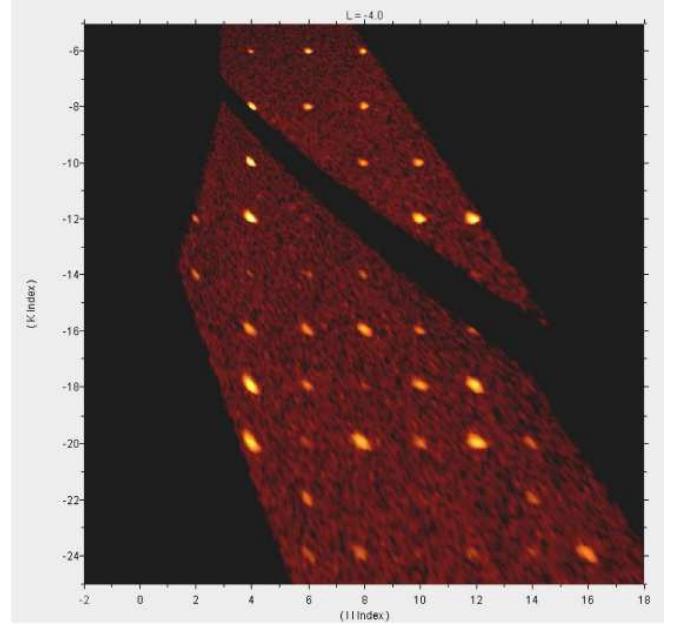


FIG. 5: (Color online) Diffraction data for $\text{TbFe}_2\text{Zn}_{20}$ (s2). Representative data collected at 100 K with the SCD instrument.

TABLE II: Basis vectors (BV) for the space group $Fd\bar{3}m:2$ with $\mathbf{k}_{-55} = (.5, .5, .5)$. The Tb atoms of the nonprimitive basis are defined according to 1: (.125, .125, .125), 2: (.875, .875, .875).

IR	BV	Atom	BV components					
			$m_{\parallel a}$	$m_{\parallel b}$	$m_{\parallel c}$	$im_{\parallel a}$	$im_{\parallel b}$	$im_{\parallel c}$
Γ_2	ϕ_1	1	1	1	1	0	0	0
		2	1	1	1	0	0	0
Γ_3	ϕ_2	1	1	1	1	0	0	0
		2	-1	-1	-1	0	0	0
Γ_5	ϕ_3	1	1	-0.5	-0.5	0	0	0
		2	-1	0.5	0.5	0	0	0
	ϕ_4	1	0	0.866	-0.866	0	0	0
		2	0	-0.866	0.866	0	0	0
Γ_6	ϕ_5	1	1	-0.5	-0.5	0	0	0
		2	1	-0.5	-0.5	0	0	0
	ϕ_6	1	0	0.866	-0.866	0	0	0
		2	0	0.866	-0.866	0	0	0

From the resistivity data, the calculated Residual Resistivity Ratio (RRR) for samples s1 and s2 are $\text{RRR}(s1) \approx 26.3$ and $\text{RRR}(s2) \approx 5.5$. The Residual Resistivity Ratio is the ratio between the low temperature electrical conductivity (e.g. at 2 K below the boiling point of liquid helium) and the room temperature electrical conductivity, $\text{RRR} = \sigma_{2K} / \sigma_{300K} = \rho_{300K} / \rho_{2K}$. Because the room temperature electrical conductivity is primarily due to phonon scattering, whereas the low temperature electrical conductivity is primarily due to disorder scattering, therefore the lower T_c observed for s2 may be associated with the lower RRR value (higher disorder) of s2.

Neutron diffraction data for s1 and s2 were collected at 100 K (Fig.5). Data were also collected at 20 K for s2 to examine the magnetically ordered state. The previous crystallographic data reported by Nasch *et al.*²⁰ determined from single crystal x-ray scattering experiments were used as starting parameters for structural refinements. The subsequent refinements confirmed the $\text{CeCr}_2\text{Al}_{20}$ type structure and produced nearly identical atomic positions, but with small differences in the atomic site occupancies which may indicate a slight zinc deficiency in the samples studied here ($< 1.5\%$). The small χ^2 and residual values reported in Table III indicate that these refinements are of high quality.

Table III summarizes the refined lattice parameters, atomic positions and site occupations of s1 and s2. No difference was found between the lattice parameters and atomic positions of s1 and s2. Moreover, the refinements indicate that differences in the atomic site occupations are at the level of 3σ , although both samples appear to have a slight Zn deficiency. Hence, we are able to conclude that any differences in site occupancy are indeed quite subtle. Here we note that in contrast to the x-ray cross-sections for Fe and Zn, the neutron cross-sections for Fe and Zn are differ by a factor of ~ 2.8 . The anisotropic thermal parameters of s1 and s2 at 100 K are compared in table IV. The refinement results indi-

cate universally smaller thermal parameters for s1 than for s2. The thermal parameters are sensitive to disorder and hence the difference between the two sets of thermal parameters suggests that s2 is slightly less ordered than s1 consistent with the experimental observation that s2 exhibits a lower ordering temperature. However, given the quality of the refinements the level of disorder is expected to be small.

s2 was measured at 20 K to examine the magnetically ordered state. The results of structural refinements including a magnetic moment on Tb site are shown in Table III. For consistency the atomic fractions were restricted to the 100 K value. As at higher temperatures the residuals and χ^2 indicate high quality refinements. An ordered moment of $6.01(5) \mu_B$ on the Tb site was given by the fits. Since the ordered moment would not be fully saturated at 20 K a larger fraction of the full Tb moment should be recovered at low temperature. We also attempted to refine a moment on Fe in the ordered state. The refinements were not robust, but a moment of less than $1 \mu_B$ improved χ^2 slightly. Further experiments that can collect data at low Q values and hence are more sensitive to the sharper fall off of the Fe form factor are required to explicitly verify this possibility.

IV. DISCUSSION

In the $\text{RT}_2\text{Zn}_{20}$ compounds, the rare earth and transition metal ions are surrounded by Zn cages preventing direct exchange interactions between the $4f$ levels or the $3d$ levels. Rather, an indirect exchange interaction mediated by the conduction electrons, referred to as the Ruderman-Kittel-Kasuya-Yosida (RKKY)²¹⁻²⁴ exchange interaction provides the mechanism for the magnetic order. Therefore, the number of conduction electrons plays an important role in determining the magnetic properties of the $\text{RT}_2\text{Zn}_{20}$ compounds. The remarkable differences in magnetic behavior between $\text{TbCo}_2\text{Zn}_{20}$ and $\text{TbFe}_2\text{Zn}_{20}$ can be associated with the fact that there are two extra electrons per formula unit in $\text{TbCo}_2\text{Zn}_{20}$ than in $\text{TbFe}_2\text{Zn}_{20}$. Our neutron diffraction data show explicitly that the magnetic interactions have changed profoundly going from the ferromagnetic interactions in $\text{TbFe}_2\text{Zn}_{20}$ to antiferromagnetic interactions in $\text{TbCo}_2\text{Zn}_{20}$. This is consistent with the band structure calculations¹, which indicate higher d -electron density of states at the Fermi level for the $\text{RFe}_2\text{Zn}_{20}$ compounds than the $\text{RCo}_2\text{Zn}_{20}$ analogues that result in a FM ground state for the $\text{RFe}_2\text{Zn}_{20}$ compounds and an AFM ground state for the $\text{RCo}_2\text{Zn}_{20}$ compounds.

$\text{TbCo}_2\text{Zn}_{20}$ orders at $T_N \approx 2.5$ K which is as expected due to the very low rare earth concentration and the large distance between R-R ions in the $\text{RT}_2\text{Zn}_{20}$ series, the shortest R-R spacing is $\sim 6\text{\AA}$. However, local moment bearing $\text{RFe}_2\text{Zn}_{20}$ compounds exhibit high ordering temperatures ($T_C \approx 86, 66, 46$ K for R = Gd, Tb, and Dy respectively). It has been proposed

TABLE III: Single-crystal structural refinement results for TbFe₂Zn₂₀

Atom	S#	<i>x</i>	<i>y</i>	<i>z</i>	fraction
Tb (8 <i>a</i>)	s1 100 K	0.125	0.125	0.125	1
	s2 100 K	0.125	0.125	0.125	1
	s2 20 K	0.125	0.125	0.125	1
Fe (16 <i>d</i>)	s1 100 K	0.5	0.5	0.5	1.006(3)
	s2 100 K	0.5	0.5	0.5	0.986(4)
	s2 20 K	0.5	0.5	0.5	0.986
Zn1 (16 <i>c</i>)	s1 100 K	0	0	0	0.976(4)
	s2 100 K	0	0	0	0.993(5)
	s2 20 K	0	0	0	0.993
Zn2 (48 <i>f</i>)	s1 100 K	0.48932(2)	0.125	0.125	0.993(3)
	s2 100 K	0.48923(2)	0.125	0.125	0.979(4)
	s2 20 K	0.48920(4)	0.125	0.125	0.979
Zn3 (96 <i>g</i>)	s1 100 K	0.05884(1)	0.05884	0.32620(1)	0.991(3)
	s2 100 K	0.05886(1)	0.05886	0.32612(2)	0.986(3)
	s2 20 K	0.05885(2)	0.05885	0.32611(2)	0.986
Lattice cell/ Reliability factors	s1 100 K	<i>a</i> =14.049(2) Å; <i>V</i> _{cell} =2772.9(7) Å ³ R=5.7 %; R _w =5.3 %; χ ² =2.7;			
	s2 100 K	<i>a</i> =14.049(3) Å; <i>V</i> _{cell} =2772.9(9) Å ³ ; R=6.4 %; R _w =6.3%; χ ² =2.1 ;			
	s2 20 K	<i>a</i> =14.038(3) Å; <i>V</i> _{cell} =2766.4(9) Å ³ ; R=6.0%; R _w =6.7%; χ ² =2.4; <i>M</i> _{20K} = 6.01(5)μ _B			

TABLE IV: Anisotropic Thermal Parameters for TbFe₂Zn₂₀

Atom	s#	100*U11	100*U22	100*U33	100*U12	100*U13	100*U23
Tb (8 <i>a</i>)	S1 100 K	0.297(11)	0.297	0.297	0	0	0
	S2 100 K	0.329(12)	0.329	0.329	0	0	0
Fe (16 <i>d</i>)	S1 100 K	0.345(6)	0.345	0.345	-0.011(5)	-0.011	-0.011
	S2 100 K	0.370(7)	0.370	0.370	-0.024(5)	-0.024	-0.024
Zn1 (16 <i>c</i>)	S1 100 K	0.715(12)	0.715	0.715	-0.135(9)	-0.135	-0.135
	S2 100 K	0.807(13)	0.807	0.807	-0.135(9)	-0.135	-0.135
Zn2 (48 <i>f</i>)	S1 100 K	0.452(10)	0.428(7)	0.428(7)	0	0	-0.075(7)
	S2 100 K	0.496(11)	0.452(8)	0.452(8)	0	0	-0.080(8)
Zn3 (96 <i>g</i>)	S1 100 K	0.608(5)	0.608	0.464(7)	-0.143(6)	-0.019(4)	-0.019(4)
	S2 100 K	0.661(6)	0.661	0.517(8)	-0.145(6)	-0.020(4)	-0.020(4)

that the 3*d* electrons from Fe sites act as important mediators for the R-R interaction in RFe₂Zn₂₀ system regardless of the details of the mechanism involved in this interaction^{23,24}, and the interaction between Fe 3*d* electrons enhances the magnetic interaction between R³⁺ local moments, resulting in the remarkably high *T*_C for RFe₂Zn₂₀. This scenario is supported by the band structure calculation results which predicts ~ 0.67 μ_B induced Fe moment in the ground state of GdFe₂Zn₂₀^{1,4}. In particular, high sensitivity of *T*_C to the small sample-to-sample variation has been observed in RFe₂Zn₂₀. Careful structural refinements of the two TbFe₂Zn₂₀ samples s1 and s2 show no obvious site disorders, but do show small differences in thermal parameters for the two samples studied here. The refinement results suggest that s2 is slightly more disordered than s1 as indicated by the larger thermal parameters determined for s2. This is in good agreement with the resistivity data which exhibits a lower RRR value for s2. It is

not typical that such small amount disorder would so drastically affect the *T*_C. The ~ 15 K difference in *T*_C observed for s1 and s2 may be related to the proximity of the RFe₂Zn₂₀ compounds to the Stoner limit, and their associated greatly enhanced band magnetism. As also demonstrated in doping studies^{1,3}, the enhanced magnetism is extremely sensitive to disorder so that even very small amounts of disorder could significantly change the Curie temperature.

Acknowledgments

We would like to thank V. O. Garlea for helping with the TbCo₂Zn₂₀ magnetic structure refinement. Ames Laboratory is operated for the U.S. Department of Energy by Iowa State University under Contract No. DE-AC02-07CH111358. Work at ORNL was supported by the Scientific User Facility Division, office of Basic Energy Science, DOE. Work at Argonne National Labo-

ratory was supported by the U.S. Department of Energy, Office of Science, Office of Basic Energy Sciences, under

contract DE-AC02-06CH11357.

-
- * Present address: Department of chemistry, Princeton University, Princeton, NJ 08544, USA
- ¹ S. Jia, S. L. Bud'ko, G. D. Samolyuk, and P. C. Canfield, *Nature Physics* **3**, 334-338 (2007)
 - ² M. S. Torikachvili, S. Jia, E. D. Mun, S. T. Hannahs, R. C. Black, W. K. Neils, Dinesh Martien, S. L. Bud'ko, and P. C. Canfield, *PNAS* **104**, 9960-9963 (2007). www.pnas.org/cgi/doi/10.1073/pnas.0702757104
 - ³ S. Jia, Ni Ni, S. L. Bud'ko, and P. C. Canfield, *Phys. Rev B* **76**, 184410 (2007).
 - ⁴ S. Jia, Ni Ni, G. D. Samolyuk, A. Safa-Safat, K. Dennis, Hyunjin Ko, G. J. Miller, S. L. Bud'ko, and P. C. Canfield, *Phys. Rev B* **77**, 104408 (2008).
 - ⁵ S. Jia, Ni Ni, S. L. Bud'ko, and P. C. Canfield, *Phys. Rev B* **80**, 104403 (2009).
 - ⁶ Verena M. T. Thiede, Wolfgang Jeitschko, Sabine Niemann, and Thomas Ebel, *Journal of Alloys and Compounds* **267**, 23-31 (1998).
 - ⁷ O. Moze, L. D. Tung, J. J. M. Franse, and K. H. J. Buschow, *Journal of Alloys and Compounds* **268**, 39-41 (1998).
 - ⁸ Moriya, T. *Spin Fluctuations in Itinerant Electron Magnetism* (Springer, Berlin, 1985).
 - ⁹ Brommer, P. E. & Franse, J. J. M. in *Ferromagnetic Materials Vol. 5* (eds Buschow, K. H. J. & Wohlfarth, E. P.) 224 (Elsevier, Amsterdam, 1990).
 - ¹⁰ Zellermann, B., Paintner, A. & Voigtländer, J., *J. Phys. Condens. Matter* **16**, 919 (2004).
 - ¹¹ P. C. Canfield and Z. Fisk, *Philosophical Magazine Part B* **65**, 1117 (1992).
 - ¹² H. Ko, A. Safa-Sefat, S. Jia, S. L. Bud'ko, P. C. Canfield, and G. J. Miller, G. J. (2008). unpublished
 - ¹³ A. J. Schultz, P. M. De Lurgio, J. P. Hammonds, D. J. Mikkelsen, R. L. Mikkelsen, M. E. Miller, I. Naday, P. F. Peterson, R. R. Porter, and T. G. Worlton, *Physica B* **385-386**, 1059 (2006).
 - ¹⁴ [ftp://ftp.sns.gov/ISAW/](http://ftp.sns.gov/ISAW/)
 - ¹⁵ A. C. Larson and R. B. Von Dreele, *General Structural Analysis System (GSAS)*, Los Alamos National Laboratory Report LAUR 86-748 (2004).
 - ¹⁶ J. Rodriguez-Carvajal, *Physica B* **192**, 55 (1993).
 - ¹⁷ E. F. Bertaut, *J. Appl. Phys.* **33**, 1138 (1962); E. F. Bertaut, *Acta. Cryst.* **A24**, 217 (1968); E. F. Bertaut, *J. Magn. Magn. Mater.* **24**, 267 (1981).
 - ¹⁸ A. Wills, *Physica B* **276-278**, 680 (2000).
 - ¹⁹ O. V. Kovalev, *Representations of the Crystallographic Space Groups* Edition 2 (Gordon and Breach Science Publishers, Switzerland, 1993).
 - ²⁰ T. Nasch, W. Jeitschko, and U. Ch. Rodewald, *Naturforsch. B* **52**, 1023 (1997).
 - ²¹ J. J. M. Franse and R. J. Radwanski, in *Handbook of Magnetic Materials*, edited by K. H. J. Buschow (Elsevier, Amsterdam, 1993), Vol. 7, pp. 307501.
 - ²² A. Szytula and J. Leciejewicz, *Handbook of Crystal Structures and Magnetic Properties of Rare Earth Intermetallics* (CRC, Boca Raton, 1994).
 - ²³ P. G. de Gennes, *J. Phys. Radium* **23**, 510 (1962).
 - ²⁴ I. A. Campbell, *J. Phys. F: Met. Phys.* **2**, L47 (1972).